Wide-Angle Scanning and High Isolation Dual-Polarized Base Station Antennas for Sub-6 GHz Applications

Fang-Fang Fan, Pei-Pei Ma, and Qing-Lin Chen

Key Laboratory of Antennas and Microwave Technology
Xidian University, Xi'an, 710071, China
fffan@mail.xidian.edu.cn, 3305559651@qq.com, 929938860@qq.com

Abstract **–** This paper presents a wide-angle scanning and high isolation base station antenna array. The antenna element employs a compact dual-polarized umbrella-shaped printed dipole with a small size of $0.23\lambda_0 \times 0.23\lambda_0 \times 0.26\lambda_0$, which provides the possibility for a small element spacing array. The antenna element possesses wide 3 dB beamwidth of 84.6° benefiting from the pulling down of the dipole arms. Then, a dual-layer metal superstrate structure and metal wall is adopted to mitigate different kinds of mutual coupling between the dual-polarized antenna elements in the array. Owing to the wide beamwidth of the element and the low mutual coupling between the elements, the final 4×6 antenna array can achieve a good beam-scanning capability with maximum scanning angle up to ±55° and a small gain variation of less than 3 dB over the operation band 3.3-3.8 GHz. The fabricated array shows the measured isolation between all ports of the antennas is increased to more than 20 dB. Scanning characteristics also agree well with the simulated results. With the merits of wideband, low-cost (simple design and easy fabrication), wide-angle beam-scanning capacity, and good radiation performance, the proposed design has potential for application in 5G base station systems.

Index Terms **–** 5G base station antenna, dual-polarized antenna, high isolation, phased array antenna, wide-angle scanning.

I. INTRODUCTION

Fifth-generation (5G) communication technology has brought high data rate, large channel capacity, and low latency transmission experience to users. One of the 5G key technologies is beam-scanning arrays, which can realize multi-target communication and tracking. For 5G base station applications, dual-polarized capability should be required, which can extend system capacity without increasing size, and implement polarization diversity technology to achieve multipath fading resistance. Thus, designing a dual-polarized wide-angle scanning base station antenna array is an urgent task for researchers. To date, many efforts have been devoted to the single polarized wide beam-scanning array [1–5]. Few papers focus on both the dual-polarized and wide beam-scanning at sub-6 GHz simultaneously [6–8]. Actually, high isolation between the elements in the array is essential for wide-angle beam-scanning, otherwise serious mutual coupling would deteriorate the impedance matching and the radiation patterns of the array antennas. Single and dual-polarized array decoupling has been done recently [9–18]. Mutual coupling between the elements in the array is mainly blamed for the space wave coupling and surface wave coupling. Different decoupling methods have been used, such as DGS [9], EBG [10], and neutral line [11], which are devoted to reducing surface wave coupling. The DGS structure might introduce back radiation, and have narrow decoupling bandwidth. EBG requires more area to get better decoupling performance, which is not suitable to be used in closely packed antenna. The neutral line network needs a complicated design. Moreover, these methods are difficult to be applied in the dual-polarized antenna array. For space wave decoupling, frequency selective surface (FSS) [12], array-antenna decoupling surface (ADS) [13], meta-surface superstrate [14], baffle [15], dielectric stub [16] and hybrid decoupling array [17–18] have been employed to get better isolation.

In this paper, a dual-layer superstrate structure with periodic metal patches, referred to as a metal superstrate, has been introduced on top of the antenna to achieve distinct decoupling performance. Meanwhile, a separation metal wall is inserted between the columns of the array to reduce the cross polarization between the elements. Finally, a 4×6 antenna array is designed and fabricated. The measured results show that the mutual coupling between elements in the array is reduced to below -20 dB in the wideband range while maintaining stable radiation patterns. The array can achieve a good beam-scanning capability with maximum scanning angle up to ±55°and a small gain variation of less than 3 dB over the band 3.3-3.8 GHz.

Submitted On: April 27, 2023
Accepted On: March 16, 2024

https://doi.org/10.13052/2024.ACES.J.390208

II. DESIGN AND WORK MECHANISM

A. Antenna element configuration

Figure 1 (a) depicts the configuration of the proposed compact dual-polarized umbrella-shaped dipole. The antenna is composed of two orthogonal substrates, a microstrip balun, and two pairs of umbrella-shaped dipoles printed on both sides of the substrate. The ground plane is utilized to achieve directional radiation. The two substrates with thickness of 0.5 mm are made of FR4 with a relative dielectric constant of 4.4. Figure 1 (c) shows the detailed structure of the feeding balun. Compared with the conventional T-shaped dipole as shown in Fig. 1 (b), the proposed dipole has a more compact size, as the length of the substrate denoted *Ln1* has been reduced from 33 mm to *L1*=28 mm, which would contribute to the high isolation between the elements when the elements are formed into a compact array. Moreover, the beamwidth of the dipole has been widened from 78° to 84.6° as shown in Fig. 2 (c). Figure 2 (a) shows the simulated reflection coefficient and the port isolation. We can conclude the proposed element has a bandwidth of 14.1% (3.3-3.8 GHz) and high port isolation of more than 40 dB. The radiation patterns are stable in the whole band with the cross polarization more than 20 dB, as shown in Fig. 2 (b).

B. Antenna array decoupling scheme

With the small element distance in the array, strong coupling would deteriorate the impedance matching characteristics and the radiation patterns of the array antennas. A feasible hybrid decoupling method is employed in this paper. A separation metal wall is vertically placed between antenna elements, and a dual-layer metal superstrate structure is placed directly above the antenna array. These methods work together to realize a wideband decoupling within 3.3-3.8 GHz. The decoupling steps and mechanism will be illustrated in detail.

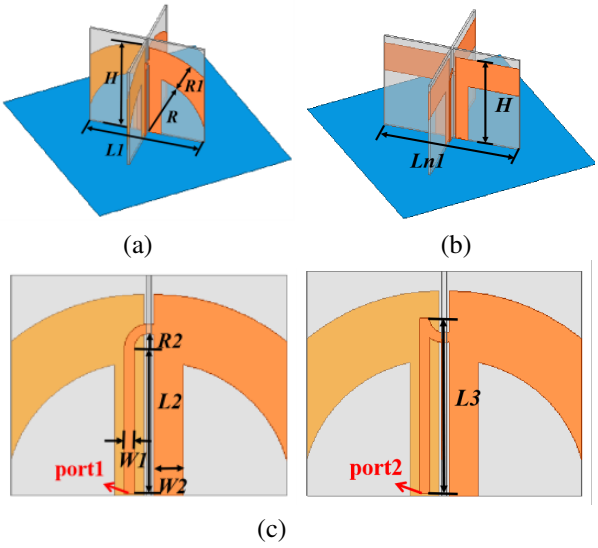

Fig. 1. Configuration of the antenna unit: (a) proposed antenna unit, (b) conventional dipole, and (c) side view of the proposed antenna (*L1*=28 mm, *R*=14 mm, *R1*=7 mm, *H*=21 mm, *Ln1*=33 mm, *R2*=2.5 mm, *L2*=15.4 mm, *W1*=1 mm, *W2*=3 mm, *L3*=18 mm).

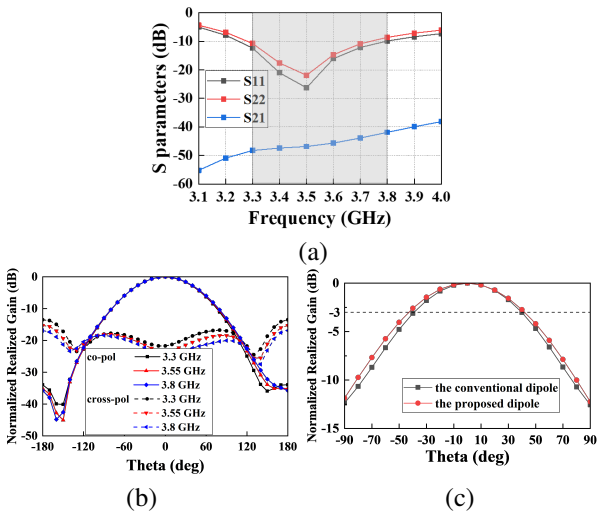

Fig. 2. Simulation results of the dipole: (a) S-parameters, (b) radiation patterns at different frequencies, and (c) comparison of the beamwidth between the conventional and the proposed dipole.

(1) Separation metal wall and lower metal superstrate for decoupling

As shown in Fig. 3 (a), it is a 1×4 linear array with the element distance of 33 mm ($0.4\lambda_0$, where λ_0 is the free space wavelength at 3.55 GHz). The port number has been marked in Fig. 3 (a). The separation metal wall is placed between two adjacent antennas, which block the propagation of spatially coupled waves and contribute to the suppression of cross-polarized coupling. The decoupling mechanism of the separation metal wall is based on the partition principle. Moreover, a lower metal superstrate is located directly on the top array as shown in Fig. 3 (b), which is used to further reduce the cross-polarized coupling between the elements. At the same time, the lower metal superstrate can also broaden the bandwidth of the antenna array. Figure 4 shows the simulated S-parameters of the 1×4 antenna array with/without the lower metal superstrate and metal wall. It is obvious that the reflection coefficients have been improved with the decoupling structure since they were deteriorating owing to the coupling, especially the higher frequency band. The co-polarized coupling achieves lower than -15 dB, and cross-polarized

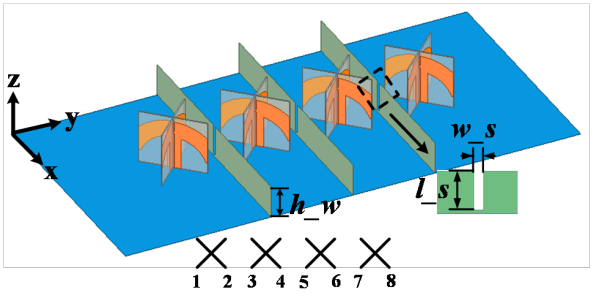

(a)

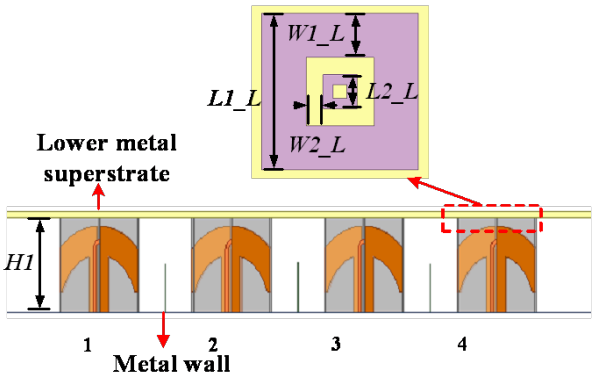

(b)

Fig. 3. The 1×4 dual-polarized antenna array: (a) with the separation metal wall and (b) with the separation metal wall and lower metal superstrate (*w_s*=2 mm, *l_s*=11 mm, *h_w*=12 mm, *W1_L*=6.5 mm, *W2_L*=1.5 mm, *L1_L*=23 mm, *L2_L*=5 mm, *H1*=23 mm).

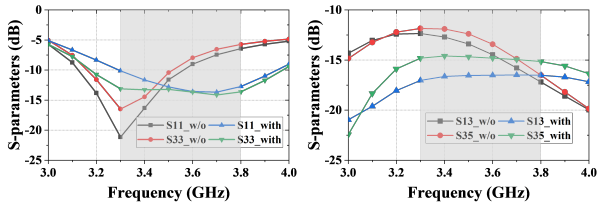

(a) (b)

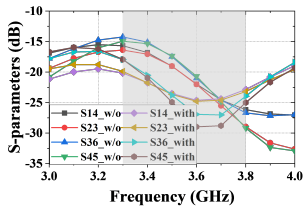

(c)

Fig. 4. S-parameters of the 1×4 antenna array with/without the separation metal wall and the lower metal superstrate: (a) reflection coefficients, (b) co-polarized coupling, and (c) cross-polarized coupling.

couplings are improved to -20 dB, almost the entire frequency band with the two decoupling structures.

(2) Upper metal superstrate for co-polarized decoupling

The addition of lower metal superstrate and separation metal wall can reduce the cross-polarized coupling to -20 dB and the co-polarized coupling to -15 dB, which cannot meet the requirements of high isolation. Therefore, the upper superstrate is employed above the array to further improve the co-polarized isolation. The distance between the ground plane and upper metal superstrate is *H2*=36.5 mm. Figure 5 shows the structure and the operating principle of the upper metal superstrate. The electromagnetic wave emitted by Antenna 1 can be reflected by the upper metal superstrate and an additional superstrate and an additional wave path is produced. When the reflected and coupling waves have the same amplitude but opposite phases, they cancel each other, reducing the mutual couplings. Figure 6 shows the simulated S-parameters of the 1×4 antenna array with/without the upper metal superstrate. It can be seen that the co-polarized coupling has been suppressed to -20 dB. Moreover, the reflection coefficients and cross-polarized coupling get better results with the upper metal superstrate. It can be observed from Fig. 7 that when an element is excited, the electric field coupled to its neighboring antenna is significantly weakened after loading the decoupling structure.

(3) Decoupling parametric study

In order to illustrate how the lower and upper metal superstrates affect the mutual coupling depression, a simulated parametric study is performed. Figure 8 (a) shows that when the parameter of the patch length

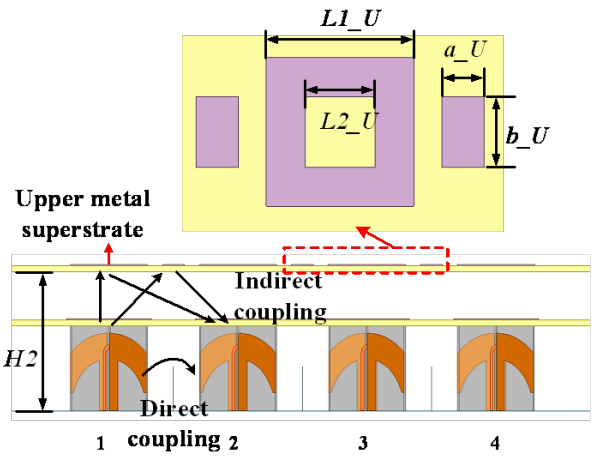

Fig. 5. The 1×4 antenna array with upper metal superstrate (*L1_U*=21 mm, *L2_U*=10 mm, *a_U*=6 mm, *b_U*=10 mm).

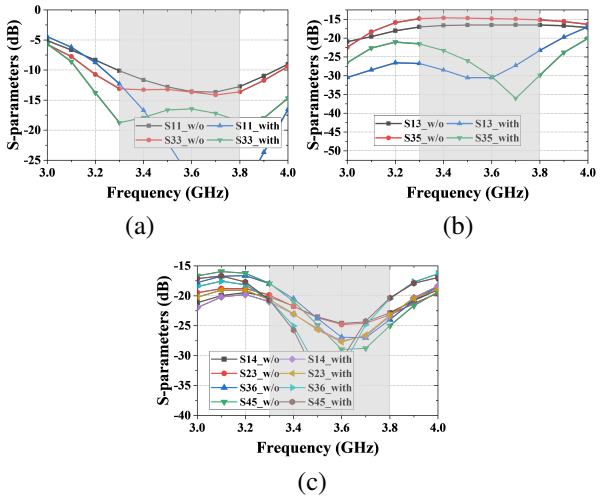

(a) (b)

(c)

Fig. 6. S-parameters of the 1×4 antenna array with/without the upper metal superstrate: (a) reflection coefficients, (b) co-polarized coupling, and (c) cross-polarized coupling.

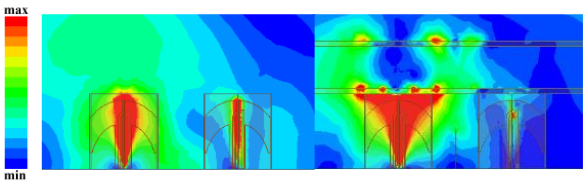

Fig. 7. Electric field distribution of the two-element array (a) without and (b) with loading decoupling structure at 3.5 GHz.

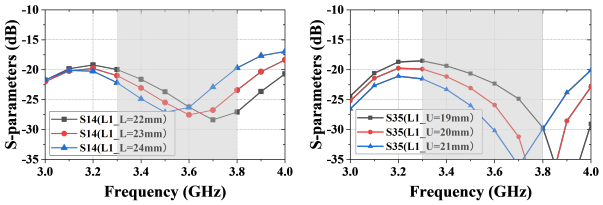

(a) (b)

Fig. 8. S-parameters of the 1×4 antenna array with and without the upper metal superstrate: (a) patch size analysis on the lower metal superstrate and (b) patch size analysis on the upper metal superstrate.

L1_L on the lower metal superstrate increases, the cross-polarization decoupling frequency point shifts to higher frequency. Figure 8 (b) shows how the parameter of the patch length *L1_U* on the upper metal superstrate influences the co-polarized decoupling. When *L1_U* increases, the co-polarized decoupling frequency point shifts to the lower frequencies. That is to say, the decoupling frequency can be controlled simply by changing the size of periodic patch cells on the superstrate.

III. ARRAY DESIGN AND RESULTS

To obtain the wide-angle scanning performance for the large-scale array, generally, the following three aspects should be considered: (a) the coupling among array elements which would lead to the scanning blindness, (b) the wide beamwidth of the array element to ensure the lower gain reduction at the large scanning angle, and (c) the small spacing to minimize the grating lobes. In this paper, the coupling has been reduced to -20 dB and the element is compact to guarantee the small spacing.

To verify the above analysis, a 4×6 array is designed. The array configuration can be seen in Fig. 9

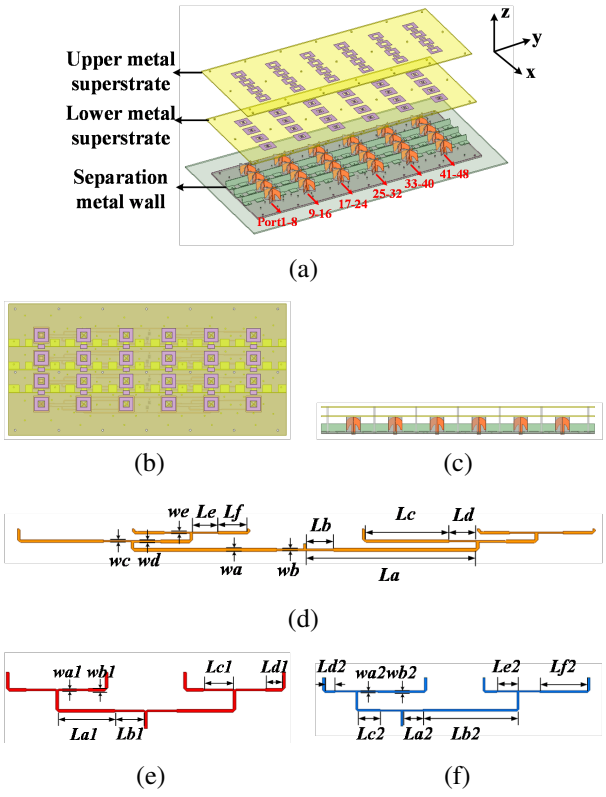

(a)

(b) (c)

(d)

(e) (f)

Fig. 9. Proposed 4×6 antenna array: (a) three-dimensional view of the model, (b) top view, (c) side view, (d) feeding network of the 4×6 array, (e) feeding network for broadside radiation, and (f) feeding network for 55° radiation (*La* = 95.96 mm, *Lb* = 15.38 mm, *Lc* = 47.3mm, *Ld* = 15.48 mm, *Le* = 14.43 mm, *Lf* = 16.6 mm, *Lb1* = *Lc1* = *La2* = *Le2* = 15.12 mm, *La1* = 28.54 mm, *Ld1* = 8.54 mm, *Lb2* = 68.64 mm, *Lc2* = 16.44 mm, *Lf2* = 33.94 mm, *Ld2* = 8.44 mm, *wa* = 1.545 mm, *wb* = *we* = 0.888 mm, *wc* = 0.61mm, *wd* = 1.13 mm, *wa1* = 0.87 mm, *wb1* = 1.56 mm, *wa2* = 0.89 mm, *wb2* = 1.56 mm).

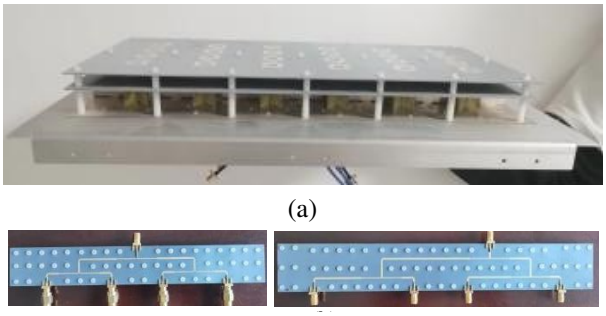

(a) (b)

Fig. 10. Photograph of (a) fabricated 4×6 antenna array and (b) fabricated power divider.

(a), the element distance in y-axis is 65 mm (0.77 λ_0, where λ_0 is the free space wavelength at 3.55 GHz). Note that power dividers used to feed the subarrays are omitted in the figure for clearer illustration. Figure 9 (a-c) illustrates the simulated model of the 4×6 antenna array and the 1 to 6 power divider model are shown in Fig. 9 (d). Figures 9 (e-f) are the 1 to 4 power dividers to feed the four subarrays in order to realize the broadside and wide-angle scanning. Figures 10 (a-b) illustrate the fabricated 4×6 antenna array model and power divider model.

The simulated and measured S-parameters are shown in Fig. 11. It is seen that the measured reflection coefficients correspond well to the simulated ones. Both the co-polarized and cross-polarized mutual coupling are reduced to below -20 dB. Figure 12 shows the simulated active reflection coefficients of the subarrays in the array

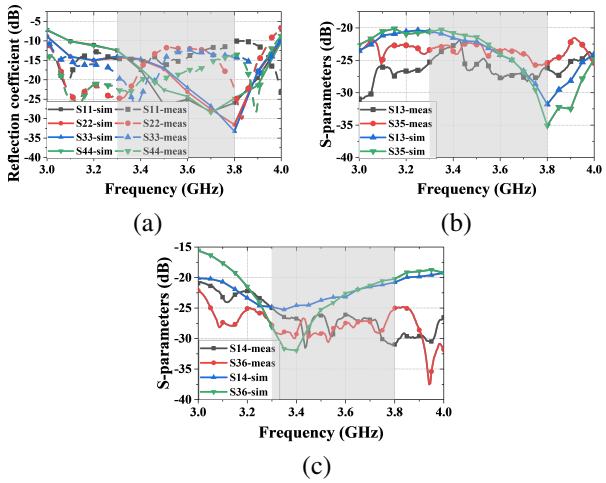

(a) (b) (c)

Fig. 11. Measured and simulated S-parameters of the 4×6 dual-polarized antenna array with the decoupling method: (a) reflection coefficient, (b) S13 and S35, and (c) S14 and S36.

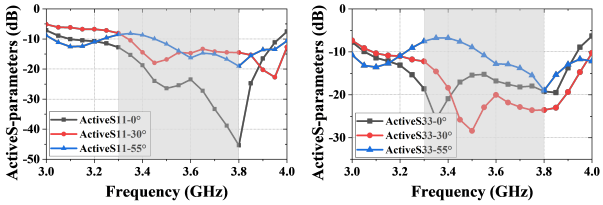

(a) (b)

Fig. 12. Simulated active reflection coefficients of the subarrays in the array and at different scanning angles: (a) port 1 and (b) port 3.

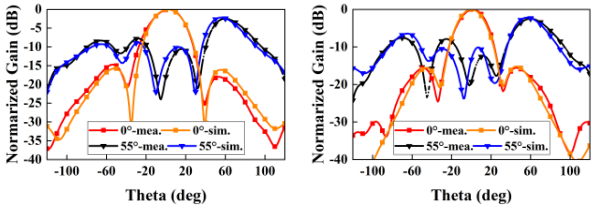

(a) (b)

Fig. 13. Simulated and measured scanning performance of the proposed array: (a) 3.3 GHz and (b) 3.8 GHz.

and at different scanning angles. It can be observed that even at wide scanning angle, the active reflection coefficients are less than -10 dB, which would guarantee the realization of wide-angle scanning. The radiation patterns and the scanning performance of the antenna array at 3.3 GHz / 3.55 GHz / 3.8 GHz are also presented in Fig. 13. It can be concluded that the main beam is able to scan up to -55° and the scan losses are lower than 2.5 dB at 3.3 GHz and 3.8 GHz. The measured and simulated realized gain are also given in Fig. 14. The measured gain is up to 19.4 dBi, which is about around 1 dB lower than the simulated gain. It may be mainly caused by fabrication and measurement errors.

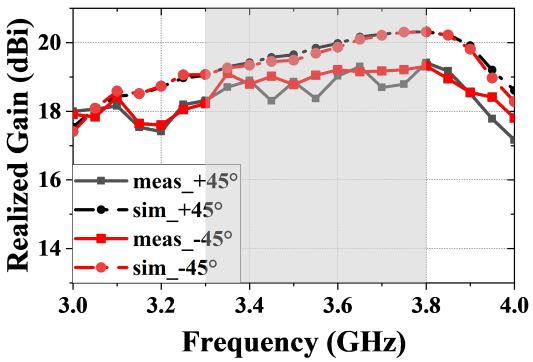

Fig. 14. Measured and simulated realized gain of the 4×6 dual-polarized antenna array.

Table 1: Comparison of the related arrays

Ref.	BW (GHz) (%)	Polarization	AS	MSA	GF	ID
[6]	4.4-5 (10.5%)	±45° dual linear	4×4	60°	3.0 dB	>20 dB
[7]	5.2-5.3 (2.1%)	dual linear	6×6	66°	3.5 dB	>16 dB
[17]	1.7-2.22 (5.6%)	±45° dual linear	4×4	-	-	>20 dB
[19]	3.3-3.8 (14.1%)	±45° dual linear	1×4	55°	>3.0 dB	>13 dB
This work	3.3-3.8 (14.1%)	±45° dual linear	4×6	55°	3.0 dB	>20 dB

BW = Bandwidth, AS = Array scale, MSA = Maximum scanning angle, GF = Gain fluctuation, ID = Inter-port decoupling

In Table 1, the comparison between our work and other antenna arrays is presented. The proposed antenna array has a broader operating bandwidth than the designs in [6–7] and [17] owing to the wideband characteristic of the proposed antenna and the decoupling structure. Meanwhile, the proposed antenna in this paper exhibits higher isolation than [19].

IV. CONCLUSION

A wide-angle beam-scanning with high isolation base station antenna array has been proposed in this paper, benefiting from the compact element and effective hybrid decoupling methods. The measured 4×6 antenna array achieved a good beam-scanning capability with maximum scanning angle up to ±55° and a small gain variation of less than 3 dB over the whole band. Plus, the measured isolation between all ports of the array is increased to more than 20 dB. With the merits of wideband, low-cost (simple design and easy fabrication), wide-angle beam-scanning capacity, and good radiation performance, the proposed design has potential for application in large-scale 5G base station systems.

REFERENCES

[1] Y. Feng, J.-Y. Li, L.-K. Zhang, X.-J. Yu, Y.-X. Qi, D. Li, and S.-G. Zhou, "A broadband wide-angle scanning linear array antenna with suppressed mutual coupling for 5G Sub-6G applications," *IEEE Antennas and Wireless Propagation Letters*, vol. 21, no. 2, pp. 366-370, Feb. 2022.

[2] S. Kim and S. Nam, "A compact and wideband linear array antenna with low mutual coupling," *IEEE Transactions on Antennas and Propagation*, vol. 67, no. 8, pp. 5695-5699, Aug. 2019.

[3] Z. Wang, Y. Dong, Z. Peng, and W. Hong, "Hybrid metasurface, dielectric resonator, low-cost, wide-angle beam-scanning antenna for 5G base station application," *IEEE Transactions on Antennas and Propagation,* vol. 70, no. 9, pp. 7646-7658, Sep. 2022.

[4] E. Adas, F. De Flaviis, and N. G. Alexopoulos, "Realization of scan blindness free finite microstrip phased arrays based on mode-free radiating electromagnetic bandgap materials," *IEEE Transactions on Antennas and Propagation*, vol. 66, no. 7, pp. 3375-3382, July 2018.

[5] G. Yang, Y. Zhang, and S. Zhang, "Wide-band and wide-angle scanning phased array antenna for mobile communication system," *IEEE Open Journal of Antennas and Propagation*, vol. 2, pp. 203-212, 2021.

[6] G. Yang and S. Zhang, "Dual polarized wide-angle scanning phased array antenna for 5G communication system," *IEEE Transactions on Antennas and Propagation,* vol. 70, no. 9, pp. 7427-7438, Sep. 2022.

[7] Y.-Q. Wen, S. Gao, B.-Z. Wang, and Q. Luo, "Dual-polarized and wide-angle scanning microstrip phased array," *IEEE Transactions on Antennas and Propagation*, vol. 66, no. 7, pp. 3775-3780, July 2018.

[8] G.-F. Gao, X. Ding, Y.-F. Cheng, and W. Shao, "Dual-polarized wide-angle scanning phased array based on multimode patch elements," *IEEE Antennas and Wireless Propagation Letters*, vol. 18, no. 3, pp. 546-550, Mar. 2019.

[9] K. Wei, J. Li, L. Wang, Z. Xing, and R. Xu, "Mutual coupling reduction by novel fractal defected ground structure bandgap filter," *IEEE Transactions on Antennas and Propagation*, vol. 64, no. 10, pp. 4328-4335, Oct. 2016.

[10] F. Yang and Y. Rahmat-Samii, "Microstrip antennas integrated with electromagnetic band-gap (EBG) structures: A low mutual coupling design for array applications," *IEEE Transactions on Antennas and Propagation*, vol. 51, no. 10, pp. 2936-2946, Oct. 2003.

[11] Y. Wang and Z. Du, "A wideband printed dual-antenna with three neutralization lines for mobile terminals," *IEEE Transactions on Antennas and Propagation*, vol. 62, no. 3, pp. 1495-1500, Mar. 2014.

[12] F. Merzaki, P. Besnier, M. Himdi, X. Castel, M. Sergolle, T. Levavasseur, and P. Caldamone, "A compact double-sided FSS absorbing wall for decoupling 5G antenna arrays," *IEEE Transactions on Electromagnetic Compatibility*, vol. 64, no. 2, pp. 303-314, Apr. 2022.

[13] C. Wei, K. Wu, X. Mei, and Z. Zhang, "Array-antenna decoupling surface," *IEEE Transactions on*

Antennas and Propagation, vol. 65, no. 12, pp. 6728-6738, Dec. 2017.

[14] J. Tang, F. Faraz, X. Chen, Q. Zhang, Q. Li, Y. Li, and S. Zhang, "A metasurface superstrate for mutual coupling reduction of large antenna arrays," *IEEE Access*, vol. 8, pp. 126859-126867, 2020.

[15] M. Li, X. Chen, A. Zhang, W. Fan, and A. A. Kishk, "Split-ring resonator loaded baffles for decoupling of dual-polarized base station array," *IEEE Antennas Wireless Propagation Letters*, vol. 19, no. 10, pp. 1828-1832, Oct. 2020.

[16] P. Mei, Y. M. Zhang, and S. Zhang, "Decoupling of a wideband dual-polarized large-scale antenna array with dielectric stubs," *IEEE Transactions on Vehicular Technology*, vol. 70, no. 8, pp. 7363-7374, Aug. 2021.

[17] B. Liu, Y. Da, X. Chen, and A. A. Kishk, "Hybrid decoupling structure based on neutralization and partition schemes for compact large-scale base station arrays," *IEEE Antennas Wireless Propagation. Letters*, vol. 21, no. 2, pp. 267-271, Feb. 2022.

[18] J. Li, H. Zhai, L. Zhao, T. Chen, Y. Wang, S. Yang, and W. Xu, "High-capacity compact massive MIMO array with hybrid decoupling scheme," *IEEE Transactions on Antennas and Propagation*, vol. 70, no. 10, pp. 9292-9304, Oct. 2022.

[19] Z. Wang and Y. Dong, "Broadband dual-polarized phased array with dynamic scanning control for intelligent mobile communication application," *IEEE Transactions on Vehicular Technology*, vol. 72, no. 10, pp. 12480-12490, Oct. 2023.

Fang-Fang Fan received a Ph.D. degree in Electromagnetic Field and Microwave Technology from Xidian University in 2011. Currently, she is an associate professor at Xidian University. Her current research interests include antenna arrays, gap waveguide technology and base station antennas for 5G application.

Pei-Pei Ma received her bachelor's degree from Hainan University in July 2019 and she is currently pursuing the master's degree at Xidian University from September 2021. Her research interests mainly concentrate on base station antennas and filters.

Qing-Lin Chen received his bachelor's degree in electronic information engineering from Xidian University, China, in July 2020. From September 2020, he studies for the master's degree in electronic and communication engineering at Xidian University, China. His current interests are to research and design millimeter wave antenna array for 5G application.